CONDENSED
MATTER PHYSICS

A Hydrogenation-Induced Nonequilibrium Oscillating Structural Transformation in Pd₃Ni Alloy

V. M. Avdyukhina*, O. V. Akimova, I. S. Levin, and A. A. Belousova

Department of Physics, Moscow State University, Moscow, 119991 Russia
*e-mail: vm_avdyukhina@physics.msu.ru

Abstract—The results of X-ray research on the structural characteristics of the Pd₃Ni alloy after its electrolytic saturation by hydrogen during relaxation are presented. The synchronous changes in the period of a lattice and the value of elastic stresses , which started immidiately after sample hydrogenation and continued for 500 hours of relaxation, were found for the first time. The observed changes are caused by the cooperative processes of the displacements of vacancies and nickel atoms between defect complexes and an alloy matrix.

INTRODUCTION

The properties of the metal–hydrogen system attract the attention of researchers who work in various fields of condensed-matter physics and physical material science due to several factors. First, dissolution of hydrogen in metals and alloys may result in the manufacture of materials with physical properties that are different from the properties of the pure metal. Second, similar investigations may clarify the question of the interaction of hydrogen with metal impurities (including crystal lattice defects). Third, Me–H systems are nonequilibrium and open under normal conditions that requires their investigations in the real-time operation mode (in situ). Because of the deficiency of the theory, it is impossible a priori to predict the character and the depth of the change in the properties of hydrogenated systems; therefore, this research aspect is urgent.

The most interesting representative of metal–hydrogen systems is the Pd–H system; interest to which is first of all caused by the high solubility and mobility of hydrogen atoms in the palladium lattice [1]. In this connection palladium and palladium-based alloys are very convenient for analyzing metal–hydrogen systems with respect to the study of their structural and kinetics properties.

Hydrogen migration during saturation and degassing, the creation of a great number of vacancies during hydrogenation, fluctuations of the phase composition, difference in the specific volumes of coexisting phases, and the different affinities of the base alloy matrix (Pd) and impurity atoms (Me) to hydrogen may result in the occurrence of various types of defects and defect complexes in hydrogen-containing palladium systems. In this connection, the most significant feature of such systems is the appearance and transformation of defect structures in them during ageing (relaxation after hydrogenation). The study of Pd–Me–H systems in this aspect has only begun [2, 3]; therefore, it is important to elucidate the character of the development of the evolution of the structure-phase characteristics of hydrogen-containing systems, the duration of its proceeding, the dependence on the initial state of systems, hydrogenation conditions, etc.

Vacancies are equilibrium defects and always are present in materials, but their concentration is small. However, hydrogen implantation into the alloy matrix may result in a significant increase in the vacancy concentration [4]. Their anomalously high concentration in metals and alloys may cause the hydrogen-induced lattice migration of atoms of alloy components, which can substantially affect the strength characteristics of such systems [5].

It should be noted that atoms of alloying metals in Pd–Me–H alloys are already primarily defects that can be distributed in the system with either order degree. Because atoms of different types have different hydrogen affinities in comparison with palladium, the hydrogen and vacancy distribution within Pd–Me–H systems may be heterogeneous and their migration direction depends on the distribution character of the component atoms and defects in the alloy matrix. Therefore, study of the hydrogen and vacancy interaction with the metal structure imperfections presents the great practical interest as well.

Table 1. The normalized intensities for the initial state and averaged for the overall states during 500 h of sample relaxation

hkl	I_{norm}, rel. units, initial state	I_{norm}, rel. units, average for 500 h of relaxation
111	3.11	3.24
200	3.54	3.83
220	6.21	5.98
311	5.40	5.18

Table 2. CSR size for different sample states

hkl	$D* 10^{-5}$ cm, initial state	$D* 10^{-5}$ cm just after hydrogenation	$D* 10^{-5}$ cm after 500 h relaxation
111	0.57	0.42	0.55
200	0.25	0.22	0.26
220	0.26	0.27	0.24
311	0.17	0.16	0.18

The characteristic feature of transition metals, to which palladium and nickel are related, is their ability to form wide regions of continuous solid solutions of implantation with hydrogen atoms [6]. They are characterized by a high rate of hydrogen diffusion that makes it possible to easily vary the concentration of Pd−Me−H solid solutions in wide limits, by varying the chemical potential of hydrogen due to an increase or decrease in its pressure during hydrogenation.

On this basis, we carried out an X-ray diffraction investigation of the behavior of the structural characteristics of the deformed Pd_3Ni alloy after its electrolytic hydrogenation during a 500-hour relaxation (ageing).

MATERIALS AND METHODS

The Pd−Ni alloy was melted from high-purity components in an electric-arc furnace. A sample was prepared by means of the grinding of part of an alloy ingot and the polishing of the formed surface; therefore, the initial state of the sample was deformed. Further, it was electrolytically saturated by hydrogen at a current density of 80 mA/cm² for 0.5 h. After hydrogenation, sample relaxation occurred in air under normal conditions. The X-ray diffraction spectra were recorded using the monochromatic Cu−$K_{\alpha1}$ radiation of a DRON-UM2 automated diffractometer. The recording and processing technique of the X-ray diffraction maxima was described in detail in [7].

RESULTS AND DISCUSSION

1. Analysis of the Structural Characteristics of the Initial State

All of the experimentally obtained quantities of the integral intensity were normalized to theoretically calculated intensities, using

$$I_{norm} = I_{rel} = \frac{I}{n_0^2 f^2 K(\theta) \exp(-2M)}, \qquad (1)$$

where n_0 is the number of unit cells in the volume unit, f is the atomic form factor, e^{-2M} is the temperature factor, and $K(\theta)$ is the polarization factor [8].

Table 1 lists the calculation results for the reduced (normalized) integral intensity for the initial state of the sample and averaged quantities of the reduced intensity for overall states during its relaxation (500 h). Because the quantities of the normalized intensities are proportional to the scattering volume, it was found (as is evident from Table 1) that the sample in the initial state has a texture in the $\langle\langle 110 \rangle\rangle$ direction.

The integral width of the diffraction lines is a characteristic of a defect material structure. If the integral widths of two orders of reflection are known, it can be traced to a variation in the size (D) of the coherent-scattering region (CSR) and the microdeformation quantities (ε) [8]. Unfortunately, the absence of experimental data on the second orders of reflection, which were not obtained because the diffraction maxima (222) and (400) had a low intensity, prevents us from determining these characteristics of the investigated alloy. Therefore, the mosaic block size was evaluated by the Selyakov−Scherrer formula [8]:

$$D = \frac{n\lambda}{\beta \cdot \cos\theta}, \qquad (2)$$

where λ is the wavelength of the X-ray radiation, θ is the diffraction angle, β is the diffraction maximum broadening, and $n \approx 0.9$. In the case of the Lorentz approximation function the diffraction maximum broadening was determined as [8]

$$\beta = B - b, \qquad (3)$$

where B is the integral width of the diffraction maximum of the sample and b is the integral width of the diffraction peak for the reference sample.

It was found that the structural components of the alloy under investigation have the sizes listed in Table 2. The errors in the determination of D are $\pm 0.01 \times 10^{-5}$ cm. From Table 2 it is evident that the size of the CSR is maximal in (111) and minimal for the CSR in (311). Sizes of the CSR in (100) and (110) are close, but half as sizes of the CSR in (111).

It was revealed that the sample under investigation in the initial state had a diffraction line spreading that was close to the CSR in (100) and (110). This means that the discrepancy in the quantities of β is caused by defects whose presence causes spreading that is pro-
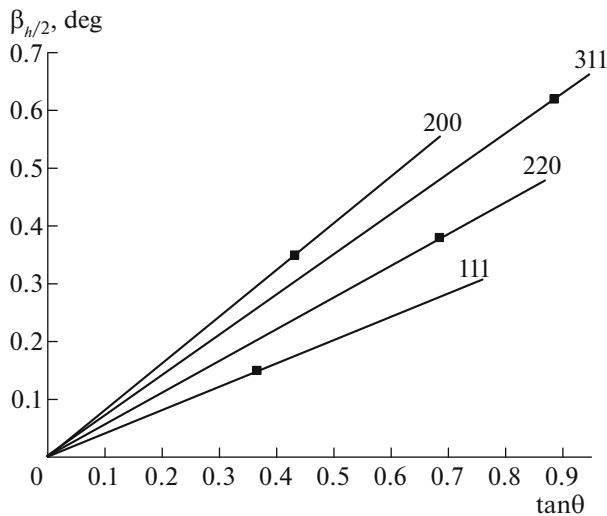
Fig. 1. The tan(θ) dependence of the diffraction-line broadening.

portional to $\tan(\theta)$ [8]. Figure 1 shows the dependence of the diffraction line broadening for the initial state of the sample on $\tan\theta$. It is evident that the line spreading in the alloy is caused by the presence of II-class defects (dislocations, their groups, dislocation walls, and dislocation loops with a long radius) because the diffraction maximum (200) broadening is greater than the maximum (111) one.

The experimentally recorded diffraction patterns of the (111), (200), (220), and (311) lines for the initial state of the sample are symmetrical curves, which are described by a single Lorentz function and had a significant width. The calculations showed that the lattice period was (3.8210 ± 0.0005) Å, which corresponds to the nickel atom concentration in the sample, (25.2 ± 0.1) at % [6], while the value of elastic stresses was negative in sign and equal to $\sigma = -(82 \pm 4)$ kg/mm^2. All this indicates that the sample in the initial state contained $D-M$ (defect−metal) complexes that had a specific volume that was greater than the alloy matrix [9]. The presence of similar defect complexes results in the appearance of elastic stresses in the sample, which is in turn characterized by the fact that the lattice parameters a_{hkl}, which are calculated from the positions of the maxima of different diffraction lines (hkl), turn out different although the crystal remains cubic as a whole.

2. The Evolution of the Structural Characteristics of the Alloy during Relaxation after Hydrogenation

The hydrogenation of the alloy did not result in the formation of a β phase that is rich in hydrogen at a current density of 80 mA/cm^2 for 0.5 h. Most likely this is connected with the fact that in the initial state the sample had sufficiently powerful defect complexes of

the $D-M$ type, which formed elastic compression stresses along the sample surface, or the $\beta \rightarrow \alpha$ transition had the high speed (completed during less than 0.4 h).

A necessary condition for the nucleation of a new phase is either a decrease of the temperature during experiment or an increase of the temperature of the phase transition [10]. Because hydrogenation occurs at room temperature, effective supercooling can be attained due to a pressure rise, which is given by the current density, j. During the electrochemical saturation the pressure is connected with the current density by the relationship

$$P(\text{atm}) = 1.7 \times 10^4 j \quad (\text{mA/cm}^2). \quad (4)$$

The applied pressure is on the order of 1360 atm at the used current density of 80 mA/cm^2. Most likely the given pressure is insufficient for the formation of nuclei of the β phase at the existing defect structure in the sample.

According to [10], the latent period for the formation of the β phase nucleus with the critical size depends on the temperature and energy of the phase transition, which is determined by expression

$$g(T) = (1 - T/T_0)q - (E_l + E_d), \quad (5)$$

where T_0 and q are the temperature and specific heat of the phase transition and E_l and E_d are the elastic energy of the formation of the nucleus of the given phase and the defect structure energy per the volume unit. The formation of the β phase is possible with the fulfillment of the condition $g(T) > 0$, which occurs under significant supercooling:

$$T_0 - T > \frac{E_l + E_d}{q}T_0. \quad (6)$$

From here it is evident that to obtain the β phase in the sample is necessary to increase the saturation-current density. An increase in the saturation time of the sample at $j = $ const only results in a rise in the initial content of the given phase. In addition, the energy of the formation of the β phase substantially depends on the energy of the defect sample structure (E_d). Because the integral width of the diffraction lines is still large enough in the initial state during the investigation of the Pd$_3$Ni alloy, the possible cause of the absence of the β phase in the sample under investigation most likely is the defect structure in it (the high "power" of the $D-M$ complexes (a great value of $|\sigma|$)).

Analysis of Table 1 shows that during the 500-hour relaxation of the sample the reduced integral intensities averaged for overall states increased for the (111) and (200) diffraction lines, which can indicate the turning of the mosaic blocks parallel to the inlet surface of the sample for CSR data, and decreased for the (220) and (311) diffraction maxima. Thus, it can be concluded that the result of the hydrogenation and
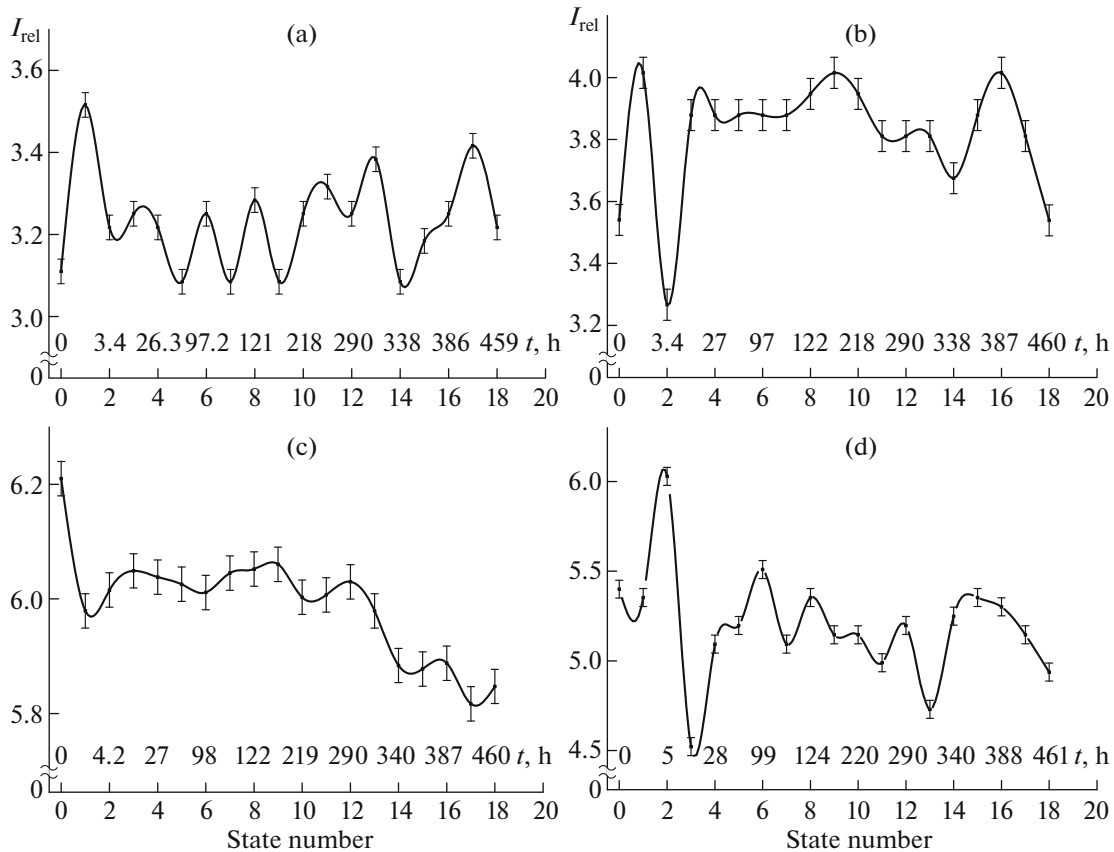
Fig. 2. The change in the integral intensity during the sample relaxation after hydrogenation (a, 111; b, 200; c, 220; d, 311).

subsequent prolonged relaxation was a decrease in the degree of the sample texture. Note that the effect was observed in hydrogenated alloys for the first time.

The calculation of mosaic blocks showed (Table 2) that just after hydrogenation the value of D decreased for (111) and (200), whereas for (220) and (311) it was practically invariable for (220) and (311). At the same time the disintegration of blocks for the CSR in (111) were maximal and reached the order of 36%. The prolonged relaxation practically restored the size of D to the value in the initial state (Table 2).

3. The Change in the Integral Intensity of Diffraction Maxima during Sample Relaxation after Its Hydrogenation

Figure 2 gives the graphs of the change in the reduced integral intensity of the (111), (200), (220), and (311) diffraction lines as a function of the relaxation time of the sample after hydrogenation and the state number.

We note that the above-mentioned dependence has an oscillating character for the overall diffraction lines; for example, for the (111) line it is evident that the normalized integral intensity increased by 13% in comparison with the initial state from the recording start to

3 h of relaxation. The 3−200 h time relaxation interval shows small oscillations of I_{rel} in the range of (3.1− 3.3) r.u. Next, at 338 h, the reduced integral intensity decreased below that in the initial state and again increased in the 338−386-h time range. As well, I_{rel} decreased at 460 h of relaxation in comparison with 338 h, but remained higher than in the initial state.

A quite different image of the dependence $I_{rel}(t)$ is observed for the diffraction maximum (200). It is evident that the value of the reduced intensity of the given line increased from the start of the recording by 13% relative to the initial state. However, I_{rel} then decreased to 3.3 r. u. (by 8% lower relative to the initial value and by 19% lower relative to a relaxation time of 2 h). At the 3.4−27 h time range, I_{rel} increased again and further remained equal within the limits of the error (3.9 r. u.) for 122 h of relaxation. In the 122−318-h time range of relaxation the reduced integral intensity decreased, oscillated weakly, and began to rise again. At 500 h of relaxation the value of I_{rel} decreased to 3.5 r. u., which was characteristic of the initial state.

The reduced integral intensity for the (220) line behaved somewhat differently: it decreased by 4% for 4 h after the sample hydrogenation. Further, it remained practically stable for a long relaxation time
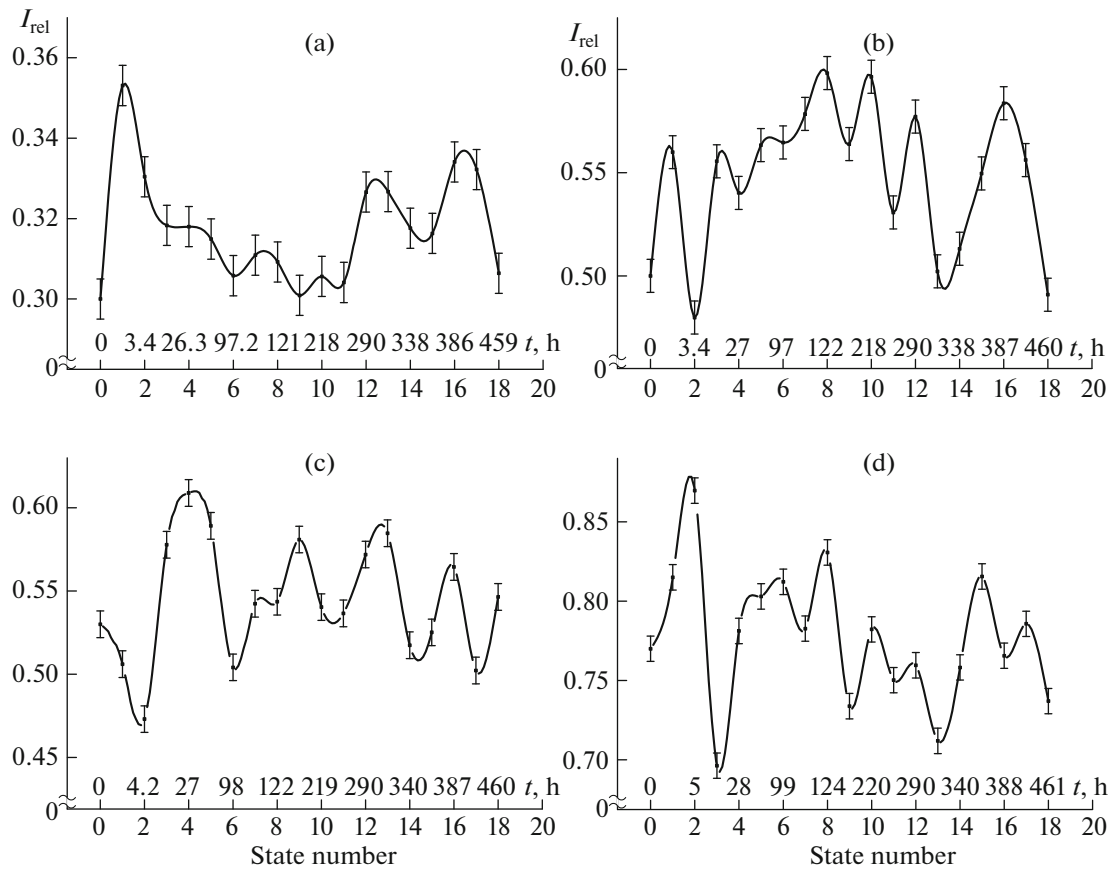
Fig. 3. The change in the integral width of the diffraction lines during sample relaxation after hydrogenation (a, 111; b, 200; c, 220; d, 311).

(4−290) h. Next, it decreased monotonically to 5.8 r.u. for the next 160 h.

The values of the reduced intensity for line (311) were practically unchanged for 5 h after the sample hydrogenation. However, in a time range of 5−24 h, I_{rel} increased to 6.0 r.u. and then abruptly dropped further. The time range of 24−99 h had a rise in I_{rel}, but significantly less than previously. After this, the value of $I_{rel}(t)$, weakly oscillated and decreased in a time range of (99−300) h and next increased again at 320−338 h. Further, the intensity dropped gradually for 50 h to 4.9 r.u., remaining lower than I_{rel} for the initial state.

4. The Change in the Diffraction Maximum Width during Sample Relaxation after Its Hydrogenation

Figure 3 shows graphs of the FWHM, full width at half maximum, $\beta_{h/2}(t)$, of the (111), (200), (220), and (311) diffraction lines as a function of the relaxation time of the sample after hydrogenation and the state number. It is evident that the dependence $\beta_{h/2}(t)$, as $I_{rel}(t)$, has an oscillating character that is dependent on diffraction line indices.

As an example, the $\beta_{h/2}$ value of the (111) diffraction line at 0.3 h of relaxation after hydrogenation of the sample increased by 17% and then gradually decreased during 240 h of relaxation (from 26.3 to 266 h). Further, $\beta_{h/2}$ still increased by two times: at 26 h and 47 h of relaxation. A decrease in $\beta_{h/2}$ to values that are characteristic of the initial states was again observed in the time range of 390−480 h of relaxation.

The form of the time dependence of the FWHM of the (200) diffraction line differs from that for (111). Just after hydrogenation at 3 h of relaxation, $\beta_{h/2}$ increased by 10%; next, at 0.5 h, it decreased practically to the initial value. Further, $\beta_{h/2}$ before 122 h of relaxation again increased by 15% in comparison with the initial width. The value of $\beta_{h/2}$ gradually decreased in the 122−330 h time range, increased in the 338−387 h range, decreased to $\beta_{h/2} = 0.48^0$, and then increased to the initial width of the diffraction line (200).

The width of the (220) line, in contrast to the other lines, first decreased by 11% and then increased by 15% relative to the initial value for 27 h of relaxation. Next, the $\beta_{h/2}$ value of the (220) line decreased to 0.50^0 at 70 h of relaxation. Further, the behavior of the change in the width of the (220) diffraction line can be
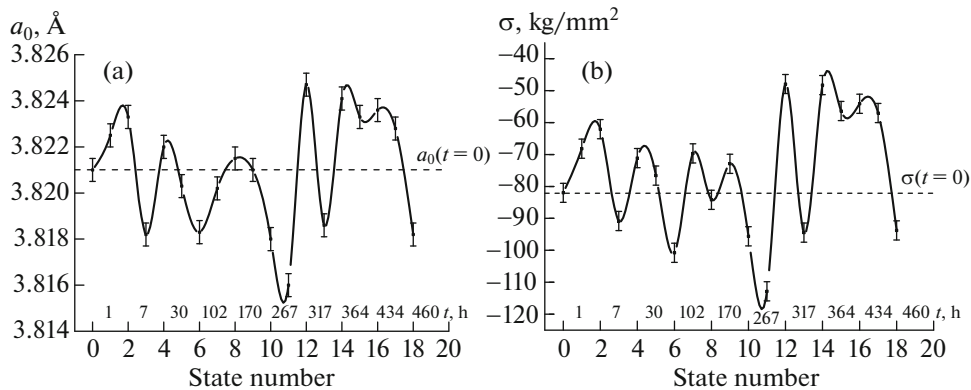
Fig. 4. The change in (a) lattice period and (b) elastic stresses during sample relaxation after hydrogenation.

called periodic: the width changed from 0.50^0 to 0.58^0 in 360 h of relaxation. At 500 h of relaxation the width of the (220) diffraction maximum was larger by 10% than for the initial state.

The integral width of the (311) diffraction line after hydrogenation increased from 0.77^0 to 0.86^0 (by 12%) in 5 h of relaxation after sample hydrogenation, $\beta_{h/2}$ then decreased to 0.68^0 at 28 h from the onset of the recording. Further, an increase in $\beta_{h/2}$ and its variation in the range of 0.78^0–0.82^0 in 95 h of relaxation occurred. A drop in $\beta_{h/2}$ to 0.72^0 followed by an increase to 0.78^0 then occurred; over another 70 h a gradual drop to 0.72^0 was observed. Next, $\beta_{h/2}$ again increased to 0.80^0 for 50 h of relaxation and then again gradually decreased to 0.74^0, which is lower than $\beta_{h/2}$ for the initial state by 4%.

Thus, it can be concluded that after the hydrogenation of this alloy, in the case of the α phase, we observed a stochastic character of value variations in both the integral intensity and the FWHM of diffraction lines. This is connected with the fact that during relaxation a change occurred in both the turning of the mosaic blocks, which are parallel to the sample surface, and in the defect structure of the α phase.

5. The Changes in the Lattice Spacing and Elastic Stresses during Relaxation of the Sample after its Hydrogenation

Because the hydrogen-rich β phase did not form in the sample, the experimental data analysis was carried out according to the phase diagram of the α phase of the Pd–Ni–H system [6]. Here, it should be noted that the phase diagram of the given system is constructed without consideration of vacancies, which enter the alloy matrix in every hydrogenation method. The vacancy concentration depends on the hydrogenation conditions. The higher the saturation current density is, the higher their concentration is in the sample.

Reuss formula [11] was used for calculation of undistorted lattice period a_o and elastic stresses σ by four diffraction lines: 111, 200, 220, and 311 for the master phase of the sample under investigation. The master phase means the most intensive component that corresponds to the diffraction peaks at their decomposition into components during relaxation after hydrogenation of the sample.

Figure 4 gives the graphs of the change in these structural characteristics. It is evident that a change in values of a_o (Fig. 4a) and σ (Fig. 4b) occurs synchronously in the overall time range. Note that such forms of the $a_o(t)$ and $\sigma(t)$ curves were first observed immediately after the sample hydrogenation, whereas Pd–Me–H (Me–Er, Mo, Ta, Hf, etc.) were characterized by the similar course of the dependences $a_o(t)$ and $\sigma(t)$ only after long-term sample relaxation, i.e., only at a small hydrogen content in the alloy matrix.

The oscillating synchronous character of the variations in the given structural characteristics can be explained by the cooperative processes of the displacement of basic impurity atoms (Ni) and vacancies between defect complexes and the alloy matrix. Because only the α phase formed in the alloy under investigation after hydrogenation, the hydrogen atom concentration, n_H/n_{Pd-Ni}, in the alloy matrix was no more than 2%. In addition, the hydrogenation was performed under a high current density; therefore, it can be assumed that the alloy matrix achieved a high concentration of vacancies, which substantially increased the diffusion mobility of the atoms of alloy components.

Let us analyze the dependence graphs in Fig. 4. It is evident that the cubic lattice period of the matrix that was calculated after the sample saturation by hydrogen increased in the first 4 hours of relaxation from $a_0 = (3.8210 \pm 0.0005)$ Å to $a_0 = (3.8233 \pm 0.0005)$ Å. This increase in the value of a_0 may be connected with several causes: the entrance of hydrogen into the alloy matrix, the outgoing vacancies that

occurred during hydrogenation, and a change in the nickel atom concentrations in the scattering layer of the sample. We will consider this question in more detail. If an increase in the lattice spacing in a time range of 0−4 h of relaxation is connected with the uptake of only hydrogen atoms into the alloy matrix, we have

$$n_H/n_{Pd-Ni} = 4.22 * \Delta a_0 \approx 0.01 = 1\%, \qquad (7)$$

which is characteristic for the α phase of practically all of the palladium-based alloys. If an increase in the lattice period is connected with the vacancy outflow from the alloy matrix, their concentration must be

$$n_{vac} = \frac{3\Delta a_0}{0.22 a_0} = 0.008 = 0.8\%, \qquad (8)$$

which is possible also because the hydrogenation of the alloy occurs at a high current density of 80 mA/cm². When it is connected with the diffusion of only impurity atoms (Ni), the nickel atom concentration in the scattering layer (with a thickness of the order of 6 μm when using Cu $K_{\alpha 1}$ radiation) must increase by 2.2 ± 0.1 at % according to the phase diagram [6].

To unambiguously determine the cause of an increase in the lattice spacing in the first hours after sample hydrogenation, let us consider the graph of the dependence of the elastic stresses on the relaxation time, which is shown in Fig. 4, b. A decrease in the "power" of the defect complexes from -82 ± 4 kg/mm² to -62 ± 4 kg/mm² in the first 4 h of the alloy relaxation indicates inflow of hydrogen and vacancies. Due to this, the diffusion mobility of Ni atoms within defect complexes increased, which promotes displacement from them into the alloy matrix. Therefore, an increase in the value of a_0 is connected first of all with the entrance of hydrogen during hydrogenation and the displacement of nickel atoms from defect complexes into the alloy matrix.

In the time range of 4−7 h of relaxation the lattice spacing of the master phase decreased to 3.8182 ± 0.0005 Å, while elastic stresses decreased to -90 ± 4 kg/mm², i.e. the "power" of the $D-M$ complexes increased by 9%. This may be connected with the fact that the majority of the vacancies moved from the defect complexes into the alloy matrix. The calculations showed that in order to create a decrease in the lattice spacing by 0.005 Å, the alloy matrix must obtained on the order of 1.6% of the vacancies, which is problematic. Because in this case a substantial increase in the "power" of the $D-M$ complexes occurred, this indicates that along with the vacancies nickel atoms enter into the alloy matrix from defect complexes and from the alloy depth. All of this provides a combined decrease in the value of a_0 and an increase in the "power" of the defect complexes that is observed in the experiment.

The oscillating behavior of the $a_0(t)$ and $\sigma(t)$ dependences was also observed in the time ranges of 7−27, 30−98, 102−123, and 123−179 h of relaxation. The deepest minimum for these dependences was recorded at a relaxation time of 267 h, when the lattice period of the master phase decreased to 3.6160 ± 0.0005 Å; and $\Delta\sigma = -40$ kg/mm². To create such a decrease in the lattice period only by vacancies that enter into the alloy matrix from defect complexes (and/or the interblock space), their concentration must be on the order of 30%, which is unrealistic. Therefore, in the given time range the general role is played by nickel atoms, which must travel into the scattering X-ray layer from the alloy depth along with the vacancies of defect complexes, which makes it easier for nickel atoms to travel to the sample surface.

In the 267−290 and 317−339 h ranges of relaxation we also observed an abrupt change in the structural characteristics, which might be explained by the displacement of vacancies from defect complexes into the alloy matrix and the displacement of nickel atoms from the depth to the sample surface and inversely. At 500 h of relaxation both the lattice period and the value of elastic stresses were lower that before the hydrogenation.

CONCLUSIONS

To explain these results, it can be supposed that during the sample hydrogenation hydrogen is firstly directed into areas with a heightened concentration of palladium atoms because they dissolve hydrogen better than nickel atoms. This results in the occurrence of hydrogen-rich thermodynamically unstable areas (clusters) of palladium. The reduction of the degree of this instability occurs because vacancies that enter the alloy matrix during hydrogenation are directed into these areas. This results in a vacancy deficiency in the nickel-rich areas of the matrix; this is the driving force for the inverse vacancy flow. The result of the combination of these processes is both variations in the diffraction maximum intensity and its abrupt "disruption." The latter may be connected with the periodic (but with a large period) appearance of vacancy dislocation loops with a radius that provides both the spreading of diffraction maxima (increasing the halfwidth) and their abrupt weakening as well.

Thus, it can be concluded that this is the first finding of the simultaneous and sign-equal stochastic changes in the a_0 and σ values for the Pd−Ni−H alloy just after its hydrogenation and during 500 h of relaxation, which indicates the occurrence of cooperative processes of the migration of vacancies and nickel atoms predominately between the matrix and defect complexes. The displacement of alloy component atoms occurs mainly because of the entrance of vacancies into the alloy matrix during hydrogenation, which increases their diffusion mobility.

The defect complexes in the investigated alloy were stable during the 500 h of the sample relaxation; during relaxation a nonmonotonic change occurred in their "power" because of the exchange of vacancies and nickel atoms (possibly with hydrogen) with the alloy matrix.

These experimental data also showed that the positions of the diffraction peaks of the Pd−Ni−H alloy are distributed in the 2θ space quasidiscretely. One of the significant factors that determine the existence and features of this phenomenon is that the discrete character of the structural evolution was observed practically with the absence of hydrogen in the investigated alloy after hydrogenation. Therefore, it can be concluded that vacancies that entered as a result of hydrogenation and their migration during relaxation between defect complexes and the matrix are the driving force of this phenomenon.

REFERENCES

1. P. V. Gel'd, R. A. Ryabov, and E. S. Kodes, *Hydrogen and Structural Imperfections of Metals* (Metallurgiya, Moscow, 1979) [in Russian].

2. V. M. Avdyukhina, O. V. Akimova, I. S. Levin, and G. P. Revkevich, Moscow Univ. Phys. Bull. **69**, 349 (2014). doi 10.3103/S0027134914040031

3. V. M. Avdyukhina, O. V. Akimova, I. S. Levin, et al., in *Proc. Int. Seminar "Current Techniques for Studying the Structure of Materials and Their Application in Materials Science"* (Moscow, 2014), p. 21.

4. V. M. Avdyukhina, A. A. Anishchenko, A. A. Katsnelson, and G. P. Revkevich, Phys. Solid State **46**, 265 (2004).

5. D. P. Broom, *Hydrogen Storage Materials. The Characterisation of Their Storage Properties* (Springer, London, 2011).

6. Y. Sakamoto, K. Yuwasa, and K. Hirayama, J. Less-Common Met. **88**, 115 (1982).

7. V. M. Avdyukhina, O. V. Akimova, I. S. Levin, and A.A. Peganov, Moscow Univ. Phys. Bull. **70**, 37 (2015). doi 10.3103/S0027134915030029

8. V. I. Iveronova and G. P. Revkevich, *X-ray Scattering Theory* (Mosk. Gos. Univ., Moscow, 1978) [in Russian].

9. V. M. Avdyukhina, A. A. Katsnelson, and G. P. Revkevich, Platinum Met. Rev. **46**, 169 (2002).

10. A. I. Olemskoi and A. A. Katsnel'son, *Synergetics of Condensed Media* (Editorial URSS, Moscow, 2003) [in Russian].

11. Ya. S. Umanskii, *X-ray Investigation of Metals and Semiconductors* (Metallurgiya, Moscow, 1969) [in Russian].

Translated by S. Ordzhonikidze